

Full Paper

Improvements to the Aedes larvae mobile detection system

Pratana Kukieattikool^{*}, Ladawan Klinkusoom, Watcharakon Noothong, Piruin Panichphol, Porntipa Choksungnoen, Juthatip Wisanmongkol and Tanee Demeechai

National Science and Technology Development Agency, 111 Thailand Science Park (TSP), Phahonyothin Road, Khlong Nueng, Khlong Luang, Pathum Thani 12120, Thailand

^{*} Corresponding author, e-mail: pratana.kuk@nstda.or.th

Received: 6 June 2019 / Accepted: 20 July 2020 / Published: 24 July 2020

Abstract: As Aedes mosquitoes are vectors of several severe diseases, many different approaches have been used in attempts to control them. One important component of control programs is household larval surveys. To complement the labour-intensive work of these surveys, a smartphone-based approach was previously trialled; however the false alarm rate generated by this system was high. In this paper we propose an improved system architecture and a new detection algorithm for finding possible Aedes larvae blobs without the need for stabilisation and background subtraction. With this new method, the F1 score of the processing system increased by 11.33% from our previously proposed technique. In addition, we investigated the response of Aedes and Culex larvae, which can often be confused in larval surveys, and verified that our system can differentiate between the two.

Keywords: vector control, Aedes larvae detection, artificial intelligence

INTRODUCTION

Historically, millions of people have died from vector-borne diseases, and many more have suffered from their effects. The mosquito species *Aedes aegypti* and *Aedes albopictus* transmit a number of diseases including Dengue fever, Chikungunya, Zika virus and yellow fever. Dengue is considered to be the most severe mosquito-borne viral disease, and the annual number of infections has increased 30-fold over the past 50 years, to approximately 100 million worldwide [1]. Of those infections, around 500,000 are severe cases that require hospitalisation, and 2.5% are fatal. There have also been many Chikungunya outbreaks across the world over the last few decades. There are no effective treatments or vaccines for either dengue or Chikungunya. Despite the availability of an effective vaccine, there are still 200,000 yellow fever infections and 30,000 deaths annually. Although it is primarily mosquito-borne, Zika virus can also be transmitted from mother to child during

pregnancy, causing microcephaly or brain defects in some babies, and it is also associated with Guillain-Barre Syndrome in adults [2, 3]. Of 250 countries surveyed, 215 (86%), mostly in the tropics, are climatically suitable for the survival and breeding of *Aedes* mosquitoes, and more than half of these countries have reported *Aedes*-borne infections [4]. Thus, a large proportion of the world is at high risk of outbreaks of these diseases, and considerable effort is being made to control them.

Prevention of disease is a major concern of governments across the world, and while medical intervention is the main focus for many diseases, for vector-borne diseases the control of vectors provides another avenue for prevention. Strategies for managing populations of mosquito vectors may target breeding habitat, or focus on specific life cycle stages. Breeding habitat can be minimised or eliminated by using tight lids for water storage, and cleaning or emptying the water containers regularly. Larval stages can be targeted by the use of chemicals in water or by using biological control agents such as fish to feed on the larvae. Spraying insecticides can kill or reduce populations of breeding adults. Novel approaches have also been used, such as releasing genetically modified mosquitoes, or manipulating them with the *Wolbachia* bacteria [5].

Mosquito surveillance is an essential component of local integrated management programs, for measuring the success of vector control and estimating human risk. Surveillance systems involve the collection of data on disease incidence, prevalence and fatalities, verification of the presence or absence of *A. aegypti* or *A. albopictus*, identification of the type of containers used for breeding, development of maps to track larval sites in a city, collection of mosquito population data and monitoring the effectiveness of vector control [6]. From the primary data, surveillance indicators can be roughly divided into a) immature stage survey indices, b) eggs per ovitrap per week, c) female mosquitoes per sticky gravid trap per week and d) adult infection rates, and used to estimate the level of risk.

Stegomyia indices are a standard set of indices routinely used in mosquito surveys across many countries. Every water-holding container in the target area is examined and classified as positive or negative so that the House Index (HI; the percentage of houses with at least one positive container), Container Index (CI; the percentage of all container with water that is positive), Breteau Index (BI; the number of positive containers per 100 houses) and Larva Count can be calculated. These values are compared with the thresholds for each disease in each location, e.g. *Aedes* threshold values for dengue transmission in Taiwan are BI = 1.2%, CI = 1.8% and HI = 1% [7]. A study of dengue in Brazil proposed HI = 1% [8].

Because many species of mosquito larvae including *Anopheles gambiae*, *Aedes simpsoni*, *Aedes albopictus*, *Aedes aegypti* and *Culex quinquefasciatus* may live in suburban habitats, the calculation of these indices is labour-intensive and requires the knowledge and availability of experts [9]. The general procedure for larval surveys for small volume water containers (< 30 litres) is as follows: the larvae are transferred from the water to white bowls for identification and counting [7]. In Thailand the local public health officers use flashlights to identify the *Aedes* larvae; a typical characteristic of the *Aedes* larvae is that they are more sensitive to changes in light intensity than *Culex* larvae, and will immediately swim toward the bottom of a water container or to a darker area as they sense the light [10,11]. In contrast, *Culex* larvae, which are widespread and do not transmit severe diseases, respond less to the change of light intensity and spend much time filtering or resting [12]. If the officers observe any movement of larvae after exposure to the flashlight, they report the presence of the *Aedes* larvae to the surveillance system, which identifies high-risk areas for efficient vector elimination and collates all necessary information to support the dengue control and prevention strategy [13].

Other technologies are also used for tracking and monitoring *Aedes* mosquitoes and larvae, such as software, sensors, drones, electronic devices, mosquito traps/lures and biological tools [14]. The convolutional neural network (CNN) has also been applied to identify images of adult mosquitoes from the species *Aedes aegypti*, *Aedes albopictus* and *Culex quinquefasciatus* [15]. Its best testing result was obtained using GoogleNet with 76.2% accuracy. A system to lure adult mosquitoes and then detect their presence utilised the fully convolutional network (FCN) and neural-network-based regression as a classifier with an accuracy of 84% [16]. The pioneering work in automatically detecting and classifying larvae mosquitoes used a different kind of image texture descriptors such as the Local Binary Pattern, the Co-Occurrence matrix and the 2-dimensional Gabor filters to identify *Aedes* larvae using a support vector machine classifier [17]. Its best classification accuracy was 79% using 2D Gabor filters. Another system, which consisted of a smartphone, a microscope lens and a support for the smartphone, captured 60-100 times amplified larvae images and differentiated *Aedes* from other species on the basis of the comb-like scales on the eighth segment of the larvae [18]. Its classifier, using a CNN, recognised *Aedes* larvae with an accuracy of 96.88% and the other types with 64.95%. The advanced system extended the previous one by automatically cropping of the region of interest with an accuracy of 92.85% and performed classification of *Aedes* larvae positive or negative using deep neural network with an accuracy of 94.19% [18,19]. All of the methods summarised above performed with high accuracy; however, they required additional devices to capture highly magnified images, requiring more specialised skills and making the process more costly.

In order to complement the routine work of using the flashlight in identifying *Aedes* larvae, our previous work proposed a system for *Aedes* larvae surveillance system on smartphones using a well-known stabilisation and background subtraction algorithm to detect moving larvae [20]. However, the false alarm rate was high. Accordingly, we propose an improvement on the system architecture and the processing system for the detection of *Aedes* larvae in this paper. In order to confirm that the system can accurately distinguish *Culex* and *Aedes* larvae, we investigate their response to light and report the results in this paper. In the final analysis, the comparison of the proposed algorithm to our previous algorithm shows a significant improvement.

METHODS

System Overview

An overview of our improved system is depicted in Figure 1. In order to complement the routine work of using flashlight and surveyor's knowledge to identify the *Aedes* larvae, the system employs popular portable devices such as smartphones or tablets equipped with a video camera, a flashlight at the back and a location system. This system enables anyone who has the application on the device to do a survey and to report it to the *Aedes* surveillance system. On pressing the start button, the application on the smartphone will switch on the flashlight at the back and at the same time capture a 5-second video. As *Aedes* larvae are sensitive to changes of light, they will move while *Culex* larvae will stay still. The video is streamed to the video processing system, and the number of *Aedes* larvae is obtained. The number of *Aedes* larvae, together with the geolocation of the surveyor, is then sent to the surveillance server for later use. The video processing system can be implemented at the user or the server end depending on the policy. Processing at the user end on a smartphone requires great computational resources, but spares bandwidth because only the number of *Aedes* larvae and the geolocation are transmitted through the communication channel. In contrast, processing at the server

end saves computational resources at the user end but requires higher bandwidth as the whole video must be transmitted.

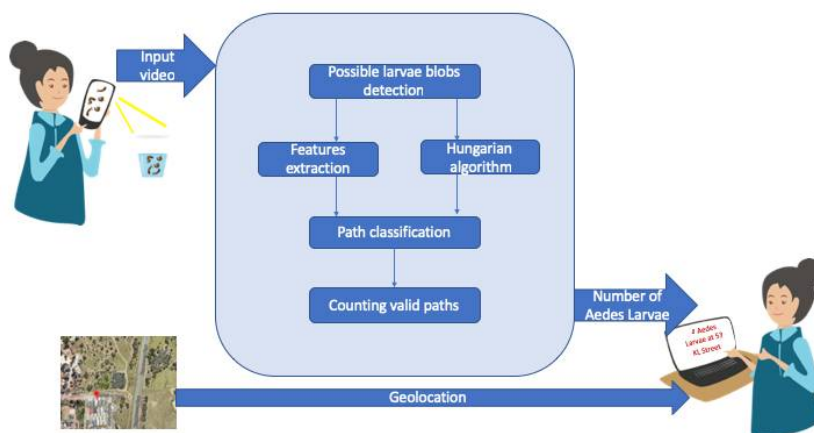


Figure 1. System overview

In previous work the video processing algorithm begins with the extraction of frames from the video, and then a reference point on each frame is aligned to stabilise the image, to eliminate shakiness in the video [20]. Background subtraction is then used to isolate the moving larvae. In this work we instead segment the images into smaller parts using an improved algorithm after frame extraction. The parts that meet our criteria we call ‘blobs’, and these are saved for later processing. The next step is the blob tracking, which assigns each blob in each frame to its respective path using the Hungarian algorithm. At the same time, the blobs with their features are classified using the Support Vector Machine (SVM) algorithm. After all the paths are obtained, the Aedes larvae moving paths are classified using the pattern-based classifier. The number of Aedes larvae moving paths are recorded as the number of the Aedes larvae present, which is then reported to the server. The method for detection of possible larvae blobs, feature extraction, the blob tracking using the Hungarian Algorithm, and the tracking path classification will be presented in more detail in this section.

Detection of Possible Larvae Blobs

The general method of moving object detection in non-fixed video cameras requires stabilisation, which is designed to eliminate image motion caused by handshaking or platform movement [21]. There are different approaches to stabilisation such as smoothing methods that use different filter types or more sophisticated approaches that estimate the motion [22-24]. Moving objects are then detected through background subtraction, which averages the whole sequence of images or generates the background model using the Mixture of Gaussians [25,26]. However, the resulting binary images obtained from the background subtraction of the stabilised images are not entirely constructed due to the non-uniform illumination. A more complicated method for detection of the moving object is to segment each object in the image using colour features, edge features and texture features. In this work we propose a new segmentation method without stabilisation, which uses image gradients to segment each object and uses colour and size as parameters for blob selection. Algorithm 1 shows the processing step to obtain the binary sub-images of the larvae (blobs). The possible larvae blobs obtained from the algorithm is depicted in Figure. 2.

Algorithm 1. Possible larvae blobs detection algorithm

Input: Frame in RGB
Output: Larvae blobs
<p>Step 1: Obtain high-gradient blobs</p> <p>1.1) Calculate the gradient magnitude of the image</p> $\ \nabla F\ = \sqrt{\ \nabla F_R\ ^2 + \ \nabla F_G\ ^2 + \ \nabla F_B\ ^2} \quad \text{where} \quad \nabla F_{R G B} = \left[\frac{\delta F_{R G B}}{\delta x}, \frac{\delta F_{R G B}}{\delta y} \right]$ <p>is the gradient of the red (R) or green (G) or blue (B) component in the x and y-direction. It provides edge strength of the image.</p> <p>1.2) Create a binary image by thresholding the gradient magnitude of the image.</p>
<p>Step 2: Exclude too big and too small blobs</p> <p>Find all 8-connected blobs of 80 to 800 pixels in the binary image which corresponds to the possible size of larvae.</p>
<p>Step 3: Exclude light-spot-like blobs</p> <p>For each blob, non-blob pixels surrounded by the blob pixels are identified. The blob may be excluded if all the identified pixels meet the following conditions: the RGB values of the pixel are all greater than 180, whereas the RGB values are represented in the range from 0 to 255, and the difference between the maximum and minimum of the three values (RGB) is less than 40.</p>
<p>Step 4: Obscure and trim the remaining blobs</p> <p>4.1) For each remaining blob, non-blob pixels surrounded by the blob pixels are included in the blob.</p> <p>4.2) Each blob is trimmed for a better representation of the possible-larva shape as follows: each blob pixel with a connection to a non-blob pixel is marked; then all the marked pixels are excluded from the blob.</p>



Figure 2. Binary image of possible larvae blobs

Feature Extraction and Classification

The features we use for classifying larval postures are the number of white pixels in a blob and the width and length of the blob frame, which can be easily extracted from binary images. Firstly, the smallest rectangular frame around each blob, which is called the blob frame, must be found. We define two features for classification of the blobs as follows:

$$Occupancy = \frac{\text{Number of white pixels in a blob}}{\text{Number of all pixels the blob frame}}$$

$$Aspect = \frac{\min(a, b)}{\max(a, b)}$$

where a and b are the width and the length of the blob frame respectively.

The postures of the larvae can be classified into two types, the straight posture class (class 1) and the bent posture class (class 2). The training of the SVM algorithm is primarily processed using human-decision on the types of blobs in the training data set, together with their features, such that we obtain a classification model for the postures of the larvae [27]. The reason behind using SVM is that it delivers the highest classification accuracy of any tested algorithm in the classification model evaluation. The types of posture obtained from the classifier model are retained for later use.

Blob Tracking by Hungarian Algorithm

In each frame of the binary image obtained in the detection step, there are several possible larvae blobs detected. We track each blob from one frame to the next, to the end of the available frames, by assigning the blob to the most probable path, so we know how each larva has changed its posture over time. The arrangement of the blobs to the tracking paths corresponds to the assignment problem that can generally be solved by the Hungarian algorithm.

The Hungarian method is a well-known combinatorial optimisation algorithm that solves the assignment problems [28]. It aims to assign n resources to n tasks on a one-to-one basis. The cost matrix C is defined as

$$C = \begin{bmatrix} c_{1,1} & c_{1,2} & \dots & c_{1,n} \\ c_{2,1} & c_{2,2} & \dots & c_{2,n} \\ \vdots & \vdots & \vdots & \vdots \\ c_{m,1} & c_{m,2} & \dots & c_{m,n} \end{bmatrix}$$

where $c_{i,j}$ is the cost of assigning the i th resource to the j th task. The steps of the Hungarian method, which attempts to find the smallest possible total cost called the optimal assignment \hat{C} , are shown in Algorithm 2 [29]. In our tracking process we assign the m tracking paths to the n newly detected blobs in the new frame using the Hungarian algorithm. At the start, all the blobs in the first frame are initialised to the m tracking paths. The Euclidean distance between the latest blob in the i th tracking path, which is located at position (x_i, y_i) , to the j th newly detected blob in the next frame, which is located at (x_j, y_j) , is calculated as:

$$c_{i,j} = \sqrt{(x_i - x_j)^2 + (y_i - y_j)^2}$$

where $i \in 1, 2, \dots, m$ and $j \in 1, 2, \dots, n$. Because the number of tracks is not always equal to the number of the newly detected blobs ($m \neq n$), there remain unmatched tracks or unassigned blobs that must be stored for the next assignment round when the next frame is processed.

Tracking Path Classification

Once the tracking paths have been found, they cannot all be declared valid Aedes larvae paths because they may represent other floating particles, or Culex larvae that did not respond to the change of light. Hence we have to classify each moving blob to determine whether it belongs to the path of moving larvae.

Algorithm 2. Hungarian method [29]

Input: C
Output: \hat{C}
Step 1: Subtract the smallest entry in each row of C from all the entries of its row, so \dot{C} is obtained.
Step 2: Subtract the smallest entry in each column of \dot{C} from all the entries of its column, so \ddot{C} is obtained.
Step 3: Draw lines through appropriate rows and columns of \ddot{C} so that all the zero entries of the cost matrix are covered and the minimum number of such lines is used. So \tilde{C} is obtained
If (the minimum number of covering lines == n) then return $\hat{C} = \tilde{C}$; else Determine the smallest of entry of \tilde{C} not covered by any line. Subtract this entry from each uncovered row, and then add it to each covered column to get the new \tilde{C} . Goto Step 3 ; end

There are many approaches to classifying the tracking path of moving objects, which mostly depend on the features of the objects of interest. For fixed-shaped objects, a method for real-time multi-vehicle tracking and counting under a fish-eye camera [30] uses low-level features and higher-level affinity-based association. The optimised Gaussian Mixture Model adjusts the Region of Interest for accurately counting the vehicles under heavy traffic conditions [31]. Another method can detect and track single small-shape-varying objects such as fruit fly larvae in response to odour, temperature and light gradients using high-resolution fixed video to determine their postures [32]. A single-sperm tracking method has been developed that can track a single object in occlusion using the likelihood obtained from the distance and velocity [33].

We deploy a pattern-based classifier to classify the paths, P , derived from the Hungarian algorithm. A pattern describes a collection of objects, which in our case is the sequence of the posture classes obtained from the SVM in the larvae classification step. Because *Aedes* larvae strongly respond to the change of light, they change their postures to move away abruptly. We can transform the fact into a process diagram as shown in Figure 3, which decides on the change of the posture classes.

The paths can be verified as *Aedes* paths if a change of posture occurs in a tracking path p_i , either from the straight posture class to the bent posture class (1->2) or vice versa (2->1). If there is only one change of posture in one tracking path, then the classifier identifies an *Aedes* larva. Algorithm 3 shows details of the process, where $P = \{p_1, p_2, \dots, p_n\}$ is the set of paths obtained from the Hungarian algorithm, $p_i = \{t_{i1}, t_{i2}, \dots, t_{im}\}$ is the sequence of posture classes in the i th path, and N is the number of *Aedes* paths. If a tracking path conforms to this rule, it is recorded as an *Aedes* larvae path. The total number of the valid paths is reported to the server as the number of observed *Aedes* larvae.

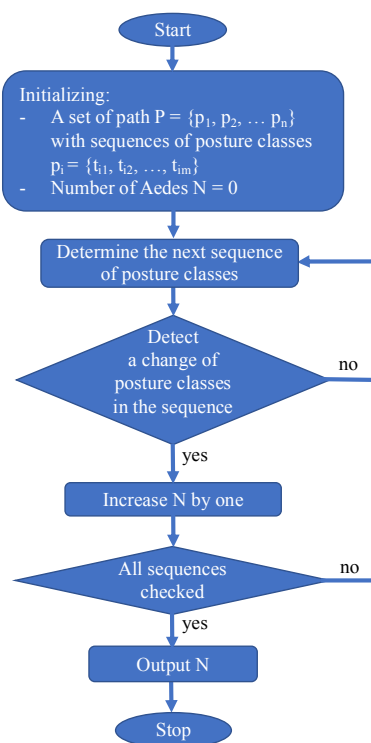


Figure 3. Process diagram for path classification

Algorithm 3. Tracking path algorithm classification

Input: P
Output: N
Initialise: $N=0$
<pre> for i = 1: n for j= 1:m-1 if (t_{ij} not equal to $t_{i(j+1)}$) then $N++$; break; end end end </pre>

RESULTS AND DISCUSSION

We performed three experiments to test the performance of the proposed system: the response of Aedes larvae and Culex larvae to the change of light, the training of the larval posture classifier, and the performance of the processing system. The results are presented below.

Response of Aedes Larvae and Culex Larvae to Change of Light

To verify the different reactions of the Aedes larvae, which are our target for detection, and Culex larvae, which are not, we put a sample of ten Aedes larvae and ten Culex larvae in separate

bowls for observation. We used our smartphone application to turn on the flashlight and recorded a video.

Figure 4 shows consecutively nine frames of a video file, which recorded an *Aedes* larva immediately after the light was turned on. It can be seen that the larva changes its posture from straight to bent posture in these nine frames. This response was seen in all ten *Aedes* larvae. In Figure 5 the nine frames of a video file recording a *Culex* larva immediately after the light was turned on show no change of posture. This was consistent for all ten *Culex* larvae.



Figure 4. Consecutive frames of video of *Aedes* larva



Figure 5. Consecutive frames of video of *Culex* larva

The experimental results show that our proposed system of using a flashlight together with the recording of video is capable of accurately distinguishing *Aedes* larvae from *Culex* larvae. The postures of the *Aedes* larvae after exposure to the abrupt change of light also change from an s-curve to a straight to a c-curve, which are detectable using our bent and straight posture classification.

Training of Larval Posture Classifier

Training of the *Aedes* larval posture classifier was carried out using videos taken from a camera on a tripod to eliminate shaking of the video. The video was recorded with image size of 1920 x 1080 pixels, frame rate of 25 fps and colour depth of 24 bits per pixel. From each frame we extracted 291 larvae sub-images as our training samples. From these, we established occupancy and aspect, and larval postures were assessed by eye. There were 86 straight posture samples and 205 bent posture samples.

The features and the responses for the training of the larval posture classifier were processed using the SVM algorithm which has a polynomial kernel of order 2 with scale 0.3086, resulting in a total of 79% accuracy. The training was done using 5-fold cross-validation. The confusion matrix of the training of the larval posture classifier is shown in Table 1, where class 1 is the straight posture class and class 2 is the bent posture class. From the table, we calculated the performance metrics of predicting the straight posture class (class 1) with 62.63% precision, 72.09% recall, 81.95% specificity, 27.9% miss rate, 18% false alarm rate, and F_1 score of 0.6701. The reason behind the miss rate and the false alarm rate is that some of the feature values of each class lay close to each other such that the SVM hyperplane could not separate them. Also, the training samples were small and the sample sizes of the two classes unequal, which made the SVM perform with a high miss rate and false alarm rate, leading to degradation of the tracking path classification. Nevertheless, the path classification attempted to leverage this error by checking the whole sequence in order to capture at least one change of the posture classes.

Table 1. Confusion matrix of classifier for Aedes larvae postures obtained from SVM (class 1 = straight posture, class 2 = bend posture)

Predicted class	1	2
True class		
1	62	24
2	37	168

Performance of Processing System

The smartphone application for collecting video data was developed and installed on a smartphone with the manual features enabled. The focal distance of 12 cm, the exposure time of 0.004356 seconds, the ISO value of 100, the frame rate of 25 fps, and the image size of 1440 x 1080 were fixed for the flash-on environment at a selected specific distance of 12 cm. Thirty Aedes larvae were put in light-coloured containers and ten users participated in data collection to account for individual variation in filming technique and camera movement. The users attempted to hold the camera at 12 cm from the container and minimise camera-shake during recording; there were 115 files in total. We tested only the Aedes larvae without Culex larvae in the container because the Culex larvae do not change their postures, as shown in the previous experiment.

The ground-truth of all paths of moving larvae were generated by human decision and these data were used to assess the performance of the system. The measurement matrices for the correctness of the system compared to the ground-truth are precision (P) and recall (R) [34]. Recall (R) or sensitivity is the fraction of considered instances retrieved over the total number of the considered instances. In our case the considered instances that have been retrieved (TP) are the moving larvae that the system correctly detects, and the total number of considered instances ($TP + FN$) is the moving larvae in the ground-truth, where FN is the number of false negatives. Precision (P), or the positive predictive value, is the proportion of the considered instances that have been retrieved to the total number of retrieved instances, but in this case the total number of retrieved instances ($TP + FP$) is the number of moving larvae stated by the system, where FP is the number of false positives.

Optimal performance would deliver precision and recall values close to 1, but in reality the best we can do is to leverage between precision and recall. To compare the detection and tracking performance of different systems, the F-measure is deployed, which is defined as

$$F_{\beta} = \frac{(\beta^2 + 1)PR}{\beta^2P + R}$$

where β is a parameter that controls balance between precision (P) and recall (R) [35]. If $\beta = 1$, F_1 is the harmonic mean of P and R . If $\beta > 1$, the F measure places more emphasis on recall. On the other hand, if $\beta < 1$, the F-measure places more emphasis on precision. An efficient classification system has an F_1 score close to 1.

Table 2 shows the performance of the present system compared to previous methods in terms of recall, precision and F_1 scores. The results of 2D Gabor filter+SVM, AlexNet DNN and Deep Robust Network systems annotated in Table 2 are transformed into the shown performance metrics from the reported values [17-19]. These methods processed images with an magnification of 60X or more, which permitted the identification of the diagnostic character for Aedes larvae (comb-like scales on the 8th segment) used for classification. In contrast our present system relies purely on a smartphone camera and images are not magnified. Our previous method required stabilisation to remove jerky

image motion, and then the background image was constructed by averaging 20 frames [20]. After that, only the first ten frames were processed, which is equal to the number of frames processed in the present system. Moving objects were extracted by subtracting the frame from the background image and were segmented using the local threshold to obtain the possible larvae blobs. The possible blobs were filtered by size and grey-scale colour. The next steps were similar to our present system, involving path assignment with the Hungarian algorithm, blobs classification and finally path classification.

Table 2. Performance comparison of present and previous systems

Algorithm	Recall	Precision	F_1
2D Gabor filter+SVM [17]	77.41%	79.99%	0.787
AlexNet DNN [18]	100.0%	76.92%	0.870
Deep robust network [19]	94.57%	93.83%	0.942
Previous system [20]	87.66%	55.15%	0.665
Present system	81.69%	70.08%	0.741

As seen in Table 2, the systems which use magnified images have higher performance than our system, especially that using the deep robust network which has the highest recall at 94.57% and precision at 93.83% [19]. The system that uses 2D Gabor filter as a descriptor and classifies using SVM [17] has recall at 77.41% and precision at 79.99%, which is not much higher than our performance. In terms of F_1 scores, the system using deep robust network [19] performs the best and the other minuscule image processing systems [17, 18] are also better than our present system. In terms of image classification, the deep neural network [18, 19] can classify images with the highest performance but requires many training images, while SVM gives an acceptable result using a limited number of training samples. However, all of these systems require additional devices to magnify images, which increases the cost and requires special training to use.

Although our previous method [20] has higher recall than our present system ($R = 87.66\%$ vs 81.69%), it has lower precision ($P = 55.15\%$ vs 70.08%). Thus, it detects more larvae but reports more incorrectly. The superiority of the present system in terms of precision is due to a better blob detection algorithm which processes on RGB instead of only the grey-scale image of the previous system. The finer rejection of the unwanted blobs and blob shapes helps to improve the precision of the algorithm since the larval posture classifier is more effective. Another significant merit of the present algorithm is that image stabilisation is not required. The resulting F_1 score of the present system is equal to 0.741, which is around 11.33% higher than that of the previous system. However, it is still not perfect as the F_1 score is not close to 1.

The behaviour of the user is also one of several causes of classification errors in our system. For example, some people cannot estimate camera distance accurately, which means the blobs are out of the preset focal plane and illumination is insufficient. The larvae at the bottom of the container appear smaller than the preset threshold and so are filtered out, causing FN errors. The blob classifier model, which has 79% accuracy in the training, can cause errors in the final classification procedure, such as introducing more FP errors or FN errors when the classifier cannot identify the posture correctly. The Hungarian algorithm that assigns each blob to the tracking path can also be in error in the case of occlusion, where two or more blobs overlap or are very close together and so are detected as a single

blob. However, this rarely affects our system because we track the movement with only ten frames or 0.4 second so the larvae have not moved too far away from their original location.

Suggestions for Future Improvements

A more effective method for calibration of the distance between the camera and the container is required to improve the performance. The constraints of the light-coloured container should be resolved, which may require a more complex segmentation method for each frame. A more thorough classifier such as CNN and DNN may be used to improve the posture classifier performance at the cost of a more complex computation and the requirement of a greater number of balanced training samples.

CONCLUSIONS

Our system provides an alternative solution that is easy to implement and requires only a smart phone or equivalent. It is inexpensive and available to users without the need for extensive training, and will contribute to the effectiveness of wide-scale testing for the control and prevention of outbreaks of dengue fever and other mosquito-borne illnesses.

ACKNOWLEDGEMENTS

We thank the Department of Disease Control for the information on the larvae and the preparation of the larvae for our experiment. Thanks are due also to Dr. Surapa Thiemjarus for sharing her knowledge of Machine Learning and to Ms. Phattharat Songthung for sharing ideas and time discussing our results. Lastly, we thank all the anonymous reviewers whose comments help to improve and complete this work.

REFERENCES

1. World Health Organization, “A global brief on vector-borne diseases”, **2014**, http://apps.who.int/iris/bitstream/10665/111008/1/WHO_DCO_WH-D_2014.1_eng.pdf (Accessed: March 2019).
2. S. A. Rasmussen, D. J. Jamieson, M. A. Honein and L. R. Petersen, “Zika virus and birth defects — Reviewing the evidence for causality”, *N. Engl. J. Med.*, **2016**, *374*, 1981-1987.
3. World Health Organization, “Guillain–Barré syndrome”, **2016**, <https://www.who.int/en/news-room/fact-sheets/detail/guillain-barré-syndrome> (Accessed: March 2019).
4. S. Leta, T. J. Beyene, E. M. D. Clercq, K. Amenu, M. U. G. Kraemer and C. W. Revie, “Global risk mapping for major diseases transmitted by *Aedes aegypti* and *Aedes albopictus*”, *Int. J. Infect. Dis.*, **2018**, *67*, 25-35.
5. H. Gomez, N. Pavia, F. Correa, A. Martin, G. Vazquez and P. Manrique, “Challenges for the introduction and evaluation of the impact of innovative *Aedes aegypti* control strategies”, in “Dengue Fever—a Resilient Threat in the Face of Innovation” (Ed. J. A. Falcon-Lezama), IntechOpen, London, **2019**, pp.95-111.
6. US Department of Health and Human Services, “Surveillance and control of *Aedes aegypti* and *Aedes albopictus* in the United States”, **2016**, <https://www.cdc.gov/chikungunya/pdfs/Surveillance-and-Control-of-Aedes-aegypti-and-Aedes-albopictus-US.pdf> (Accessed: March 2019).

7. F. S. Chang, Y. T. Tseng, P. S. Hsu, C. D. Chen, I. B. Lian and D. Y. Chao, “Re-assess vector indices threshold as an early warning tool for predicting dengue epidemic in a dengue non-endemic country”, *PLoS Negl. Trop. Dis.*, **2015**, *9*, Art.no.e0004043.
8. R. J. Pontes, J. Freeman, J. W. Oliveira-Lima, J. C. Hodgson and A. Spielman, “Vector densities that potentiate dengue outbreaks in a Brazilian city”, *Am. J. Trop. Med. Hyg.*, **2000**, *62*, 378-383.
9. D. Aribodor, “Bionomics of mosquitoes in Anambra state, Nigeria”, *Int. J. Infect. Dis.*, **2016**, *45 (Suppl)*, 217.
10. Ministry of Public Health Thailand, “The survey and disposal of Aedes larvae in project one temple one hospital”, **2018**, https://ddc.moph.go.th/th/site/office_newsview/view/1133 (Accessed: January 2019).
11. M. Kasap, “Response of the larvae and pupae of *Aedes aegypti*, *Anopheles stephensi*, and *Culex pipiens* to light intensity changes—ii”, *Commun. Fac. Sci. Univ. Ankara*, **1978**, *22*, 33-51.
12. J. J. Skiff and D. A. Yee, “Behavioral differences among four co-occurring species of container mosquito larvae: Effects of depth and resource environments”, *J. Med. Entomo.*, **2014**, *51*, 375-381.
13. N. Sahavechaphan, M. Rattananen, P. Panichphol, W. Wongwilai, S. Iamsiri and P. Sadakorn, “TanRabad: Software suite for dengue epidemic surveillance and control”, *Int. J. Infect. Dis.*, **2016**, *53(Suppl)*, 118.
14. G. C. de Souza Silva, L. M. Peltonen, L. Pruinelli, H. Y. Shishido and G. J. Eler, “Technologies to combat Aedes mosquitoes: A model based on smart city”, *Stud. Health Technol. Inform.*, **2018**, *250*, 129-133.
15. D. Motta, A. A. B. Santos, I. Winkler, B. A. S. Machado, D. A. D. I. Pereira, A. M. Cavalcanti, E. O. L. Fonseca, F. Kirchner, R. Badaro, “Application of convolutional neural networks for classification of adult mosquitoes in the field”, *PLoS One*, **2019**, *14*, Art.no.e0210829
16. K. Kim, J. Hyun, H. Kim, H. Lim and H. Myung, “A deep learning-based automatic mosquito sensing and control system for urban mosquito habitats”, *Sensors*, **2019**, *19*, Art.no.2785.
17. Z. Garcia-Nonoal, A. Sanchez-Ortiz, A. Arista-Jalife and M. Nakano, “Comparison of image descriptors to classify mosquito larvae”, Proceedings of 17th International Conference on Computer Analysis of Images and Patterns, **2017**, Ystad, Sweden, pp.271-278.
18. A. Sanchez-Ortiz, A. Fierro-Radilla, A. Arista-Jalife, M. Cedillo-Hernandez, M. Nakano-Miyatake, D. Robles-Camarillo and V. Cuatepotzo-Jimenez, “Mosquito larva classification method based on convolutional neural networks”, Proceedings of International Conference on Electronics, Communications and Computers, **2017**, Cholula, Mexico, pp.155-160.
19. A. Arista-Jalife, M. Nakano, Z. Garcia-Nonoal, D. Robles-Camarillo, H. Perez-Meana and H. A. Arista-Viveros, “Aedes mosquito detection in its larval stage using deep neural networks”, *Knowl.-Based Syst.*, **2020**, *189*, Art.no.104841.
20. P. Kukieattikool, L. Klinkusoom, W. Noothong, P. Panichphol, P. Choksungnoen, J. Wisanmongkol and T. Demeechai, “Aedes larvae surveillance system on smartphones and algorithms”, *Inter. J. Infect. Dis.*, **2019**, *79 (suppl)*, 113.
21. C. Morimoto and R. Chellappa, “Evaluation of image stabilization algorithms”, Proceedings of 1998 IEEE International Conference on Acoustics, Speech and Signal Processing, **1998**, Seattle, USA, pp.2789-2792.
22. Y.-S. Wang, F. Liu, P. Hsu and T. Lee, “Spatially and temporally optimized video stabilization”, *IEEE Trans. Visual. Comput. Graph.*, **2013**, *19*, 1354-1361.

23. K. Uomori, A. Morimura, H. Ishii, T. Sakaguchi and Y. Kitamura, "Automatic image stabilizing system by full-digital signal processing", *IEEE Trans. Consum. Electron.*, **1990**, 36, 510-519.
24. S. Liu, L. Yuan, P. Tan and J. Sun, "Steadyflow: Spatially smooth optical flow for video stabilization", Proceedings of the IEEE Conference on Computer Vision and Pattern Recognition, **2014**, Columbus, USA, pp.4209-4216.
25. R. C. Gonzales and R. E. Woods, "Digital Image Processing", Prentice Hall, New York, **2001**, pp.626-630.
26. C. Stauffer and W. E. L. Grimson, "Adaptive background mixture models for real-time tracking", Proceeding of IEEE Computer Society Conference on Computer Vision and Pattern Recognition, **1999**, Fort Collins, USA, pp.246-252.
27. K. P. Murphy, "Machine Learning: A Probabilistic Perspective", MIT Press, London, **2012**, pp.496-504.
28. H. W. Kuhn, "The Hungarian method for the assignment problem", *Naval Res. Logist.*, **1955**, 2, 83-97.
29. D. Bruff, "The assignment problem and the Hungarian method", **2005**, http://www.math.harvard.edu/archive/20_spring_05/handouts/assignment_overheads.pdf (Accessed: October 2017).
30. W. Wang, T. Gee, J. Price and H. Qi, "Real time multi-vehicle tracking and counting at intersections from a fisheye camera", Proceedings of IEEE Winter Conference on Applications of Computer Vision, **2015**, Waikoloa, USA, pp.17-24.
31. B. Indrabayu and A. Achmad, "Gaussian mixture models optimization for counting the numbers of vehicle by adjusting the region of interest under heavy traffic condition", Proceedings of International Seminar on Intelligent Technology and Its Applications, **2015**, Surabaya, Indonesia, pp.245-249.
32. A. Gomez-Marin, N. Partoune, G. J. Stephens and M. Louis, "Automated tracking of animal posture and movement during exploration and sensory orientation behaviors", *PLoS One*, **2012**, 7, Art.no.e41642.
33. M. Ravanfar, L. Azinfar, M. H. Moradi and R. Fazel-Reyai, "Occlusion robust low-contrast sperm tracking using switchable weight particle filtering", *Adv. Sex. Med.*, **2014**, 4, 42-54.
34. D. M. W. Powers, "Evaluation: From precision, recall and F-measure to ROC, informedness, markedness & correlation", *J. Mach. Learn. Technol.*, **2011**, 2, 37-63.
35. Y. Sasaki, "The truth of F-measure", **2007**, <https://www.cs.odu.edu/~mukka/cs795sum09dm/Lecturenotes/Day3/F-measure-YS-26Oct07.pdf> (Accessed: March 2020).